

## Supporting Information

### A multicomponent interaction composite paper for triple-mode sensors and flexible supercapacitors

Jing Wei <sup>a</sup>, Youchao Teng <sup>a,\*</sup>, Taotao Meng <sup>a</sup>, Xiangting Bu <sup>a</sup>, Hongbiao Du <sup>b</sup>, Dagang Li <sup>a,\*</sup>

<sup>a</sup> College of Material Science and Engineering, Nanjing Forestry University, 159 Longpan Road, Nanjing, Jiangsu, China

<sup>b</sup> College of Environment and Natural Resources, Renmin University of China, No. 59, Zhongguancun Street, 100872 Beijing, People's Republic of China

\* Corresponding author: youchaoteng@njfu.edu.cn (Y. Teng); njfuldg@163.com (D. Li)

### Table of contents

<b>Experimental .....</b>	.S-2-3
<b>Supplementary Figures .....</b>	S-4-19
<b>Table S1-S3 .....</b>	S-20-22
<b>Reference .....</b>	.S-23-25

## **Experimental**

**Preparation of Graphene Oxide aqueous dispersion.** Graphene oxide (GO) was obtained by improved Hummer's method.<sup>1-3</sup> 1.0 g of natural graphite and 30 mL of concentrated sulfuric acid ( $H_2SO_4$ ) were added to a 150 mL three-neck round bottom flask and then stirring slowly with a Teflon paddle at 300 rpm for one h at room temperature. 3.0 g of potassium permanganate powder ( $KMnO_4$ ) was slowly added in the solution while the reaction temperature was carefully controlled to keep lower than 20 °C. 10 ml of deionized water was slowly added dropwise to the reacting system. Meanwhile, the temperature of the system raised to 98 °C for 24 h. The reaction solution was slowly added to 500 mL of deionized water, then 10 mL of 30 % hydrogen peroxide ( $H_2O_2$ ) was added dropwise to the mixture. Finally, the system turned from brown to yellow slowly. The product was washed for five times by 10% hydrochloric acid (HCl), then rinsed with deionized water to remove superfluous HCl. Finally, the product was diluted with deionized water repeatedly until the pH of the supernatant reached neutral. 10 mL of GO solution was dried by frozen drying to obtain pure GO powders.

**Synthesis of Cellulose nanofibrils.** The hydrophilic Cellulose nanofibrils (CNFs) were obtained by chemical and mechanical treatment following our reported procedures.<sup>4</sup> First, 10 g bamboo powders were treated with 6 wt.% potassium hydroxide solution at 90 °C for 2 h and then washed with deionized water until neutralized to remove hemicellulose. Second, lignin was removed using an acidified sodium chlorite solution at 75 °C for 1 h; the process was repeated five times. Finally, 1 wt.% purified cellulose slurry was passed through two grinding discs of the grinder (MKCA6-2, Masuko Sangyo Co., Ltd., Japan) at the speed of 1500 rpm to get a CNFs slurry after chemical treatment and then

the fibers were cut by reciprocating.

**Synthesis of Ti<sub>3</sub>C<sub>2</sub> (MXene).** Ti<sub>3</sub>C<sub>2</sub> layers were prepared according to a previously reported method.<sup>5,6</sup> 9 g of Ti<sub>3</sub>AlC<sub>2</sub> was slowly added into a mixture solution (1 wt.% LiF solution containing 9 M HCl) at 35 °C and the reaction could proceed under continuous stirring for 24 h to extract Al from Ti<sub>3</sub>AlC<sub>2</sub>. The resulting Ti<sub>3</sub>C<sub>2</sub> samples were washed with deionized (DI) water for five times until neutralized and centrifuged to obtain the multilayered Ti<sub>3</sub>C<sub>2</sub> sediment by DMSO. The residue was then dispersed again in DMSO for 40 h for further delamination of multilayered Ti<sub>3</sub>C<sub>2</sub> deposit. The delaminated Ti<sub>3</sub>C<sub>2</sub> layer with a dark-green supernatant solution was obtained and freeze-dried.

**Preparation of binary composite papers.** The same experimental methods fabricated RGO/CNFs, CNFs/MXene and RGO/MXene composite papers with different weight ratio, and the process has been consistent with the RGO/CNFs/MXene composite papers.

## Supplementary Figures

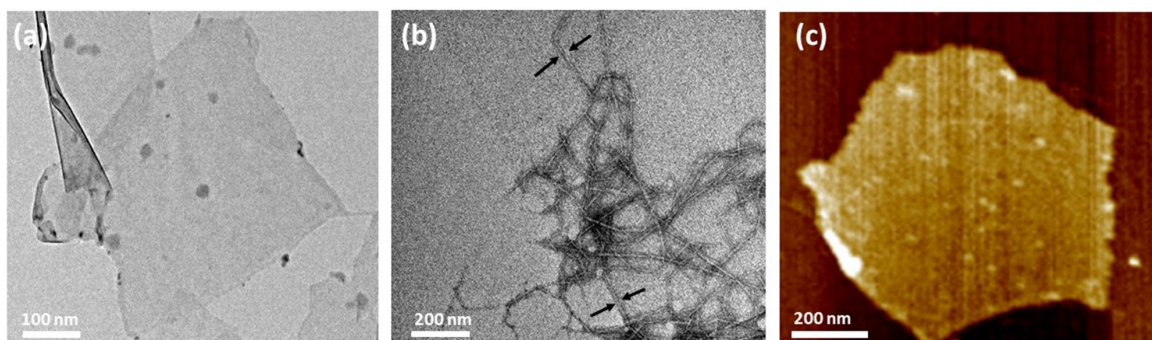


**Fig. S1** (a) TEM image of  $\text{Ti}_3\text{C}_2$  (MXene). (b) TEM image of CNFs. (c) AFM height image of GO nanosheet.

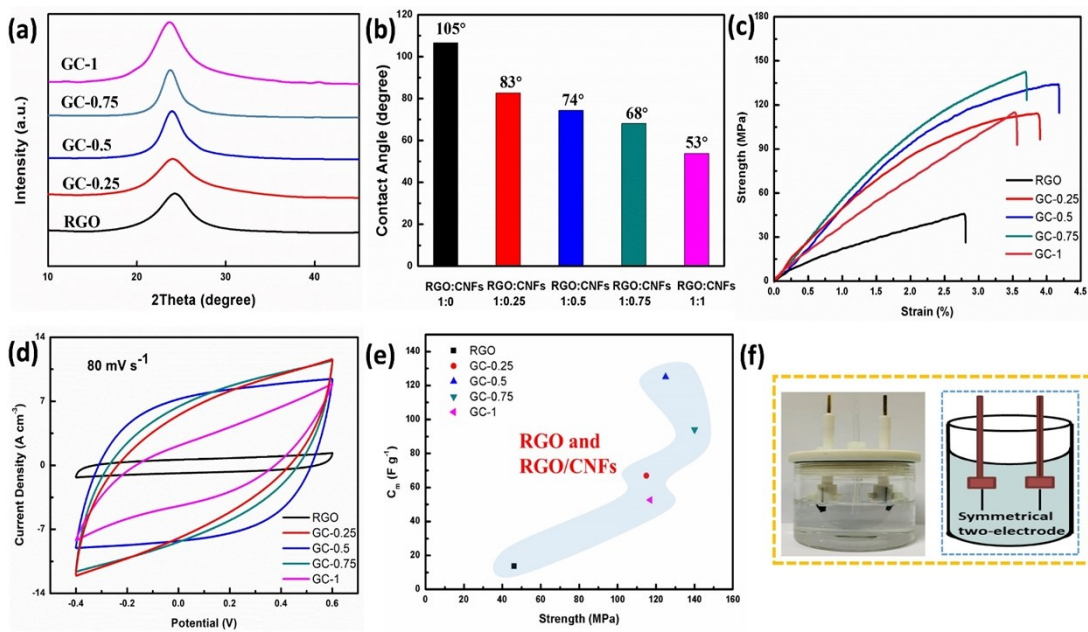


**Fig. S2** (a) Raman spectra of RGO and binary RGO/CNFs composite papers. (b) Contact angle of RGO and binary RGO/CNFs composite papers. (c) Tensile stress and strain of RGO and binary RGO/CNFs composite papers. (d) CV curves of the RGO and binary RGO/CNFs composite papers at 80 mV s<sup>-1</sup>. (e) Comparison of the gravimetric capacitance versus strength of RGO and binary RGO/CNFs composite papers with different CNFs contents. (f) The schematic diagram and photograph of the symmetric aqueous supercapacitor.

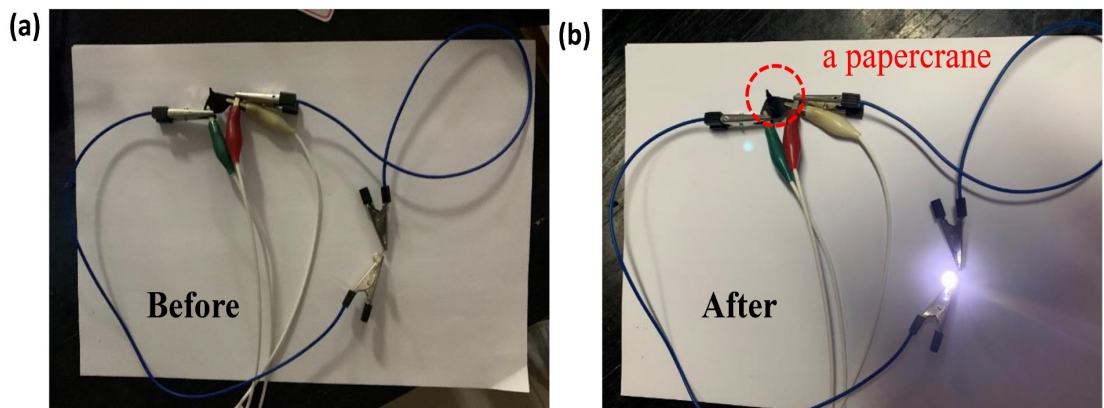


**Fig. S3** (a-b) The LED is lighted by electrochemical workstation with a paper crane (folded by flexible GCM-3 composite paper) as a conductive path.

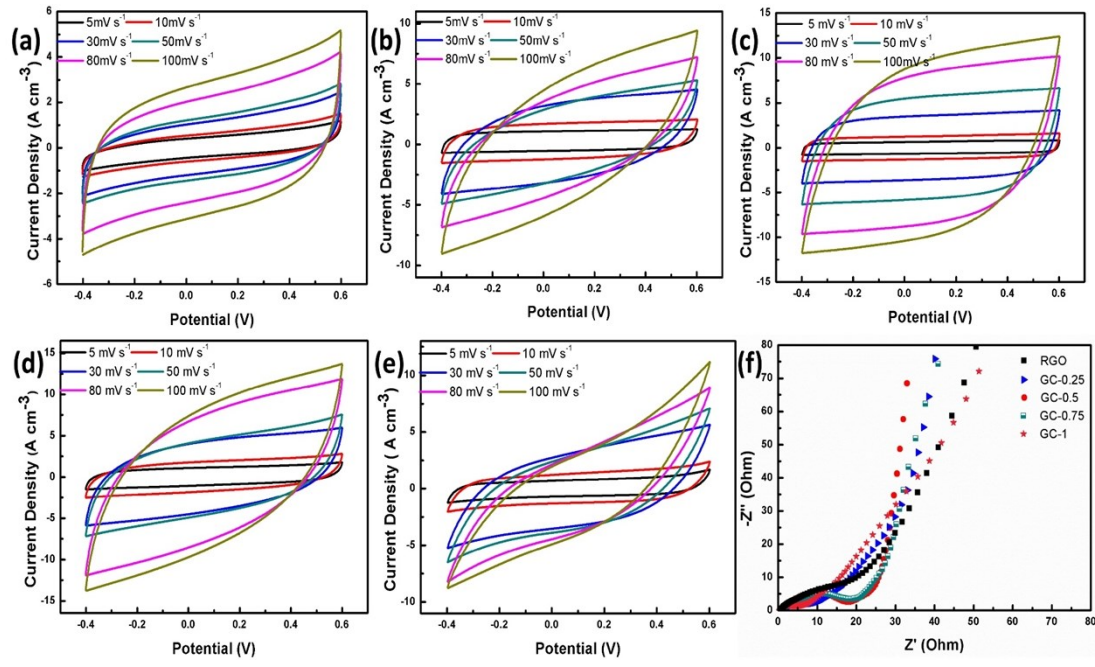


**Fig. S4** Electrochemical performance of RGO, GC-0.25, GC-0.5, GC-0.75 and GC-1 in 6 M KOH aqueous electrolyte. (a-e) CV curves, (f) Nyquist plots.

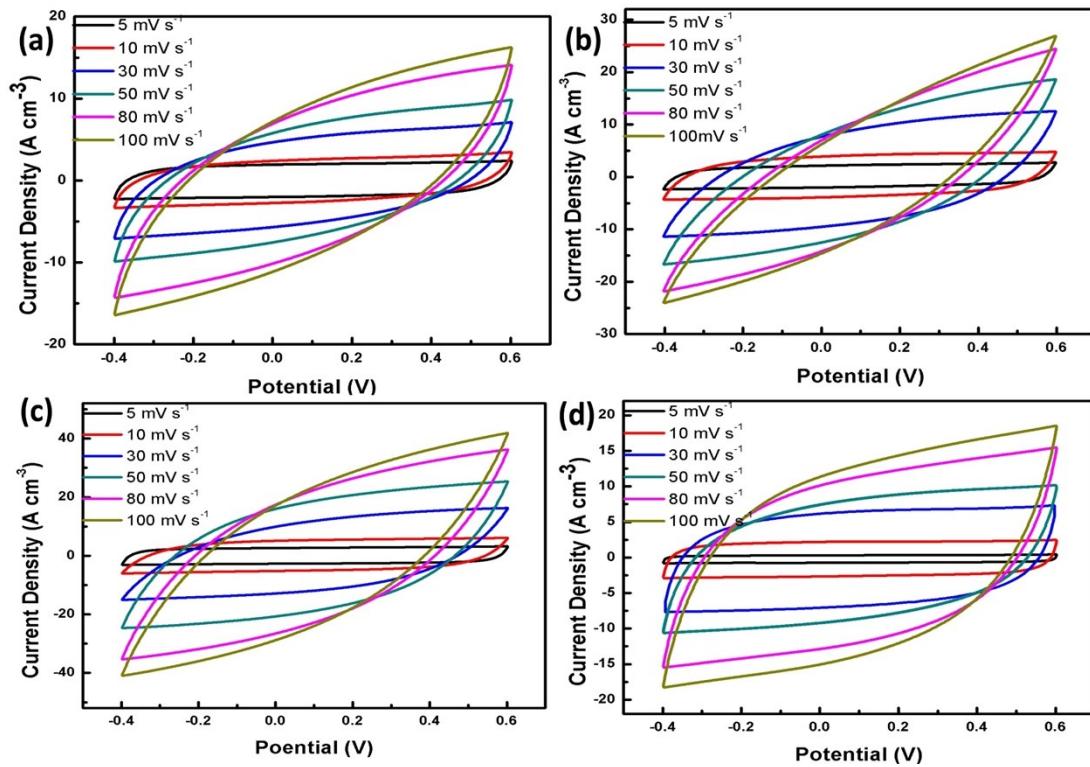


**Fig. S5** (a-d) CV curves of GCM-1, GCM-2, GCM-3, and GCM-4 composite paper in 6 M KOH aqueous electrolyte at different scan rates.

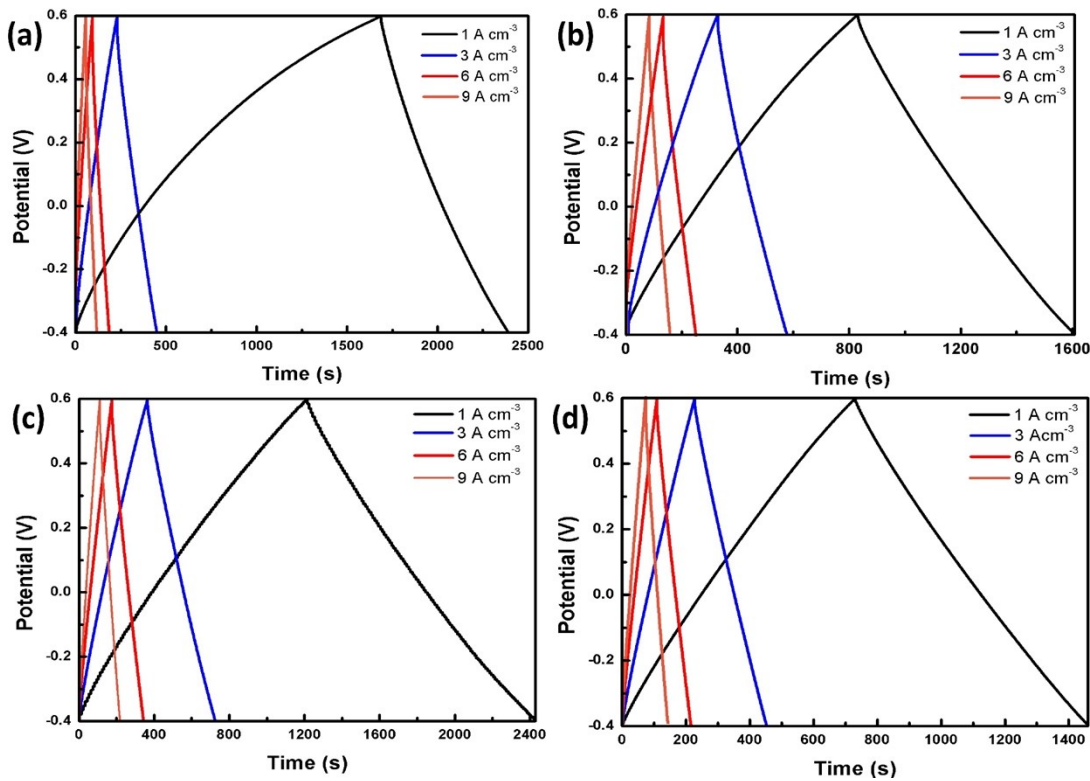


**Fig. S6** (a-d) GCD curves of GCM-1, GCM-2, GCM-3, and GCM-4 composite paper in 6 M KOH aqueous electrolyte at different scan rates.

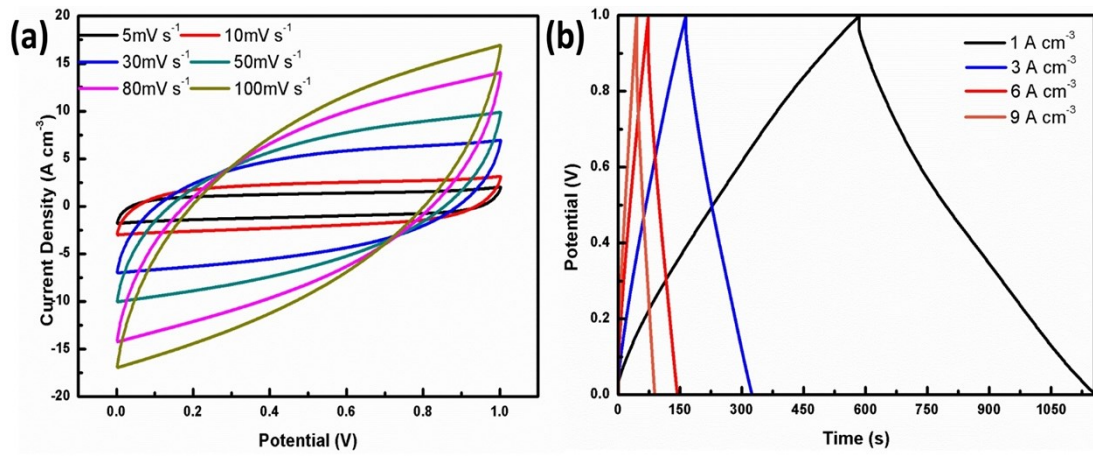


**Fig. S7** Electrochemical performance of GM-3 in 6 M KOH aqueous electrolyte. (a) CV curves at different scan rate, (b) GCD curves at different current density.

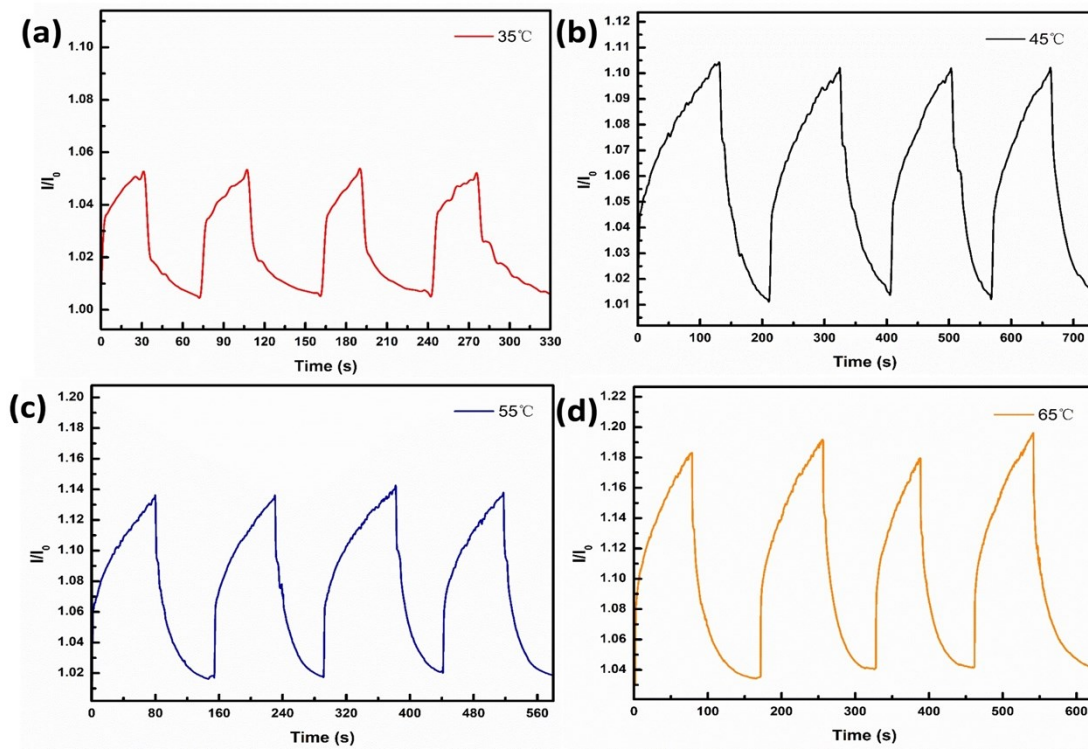


**Fig. S8** Current response of RGO/CNFs/MXene-3 stimulus response sensor under different temperature at 1V constant voltage.

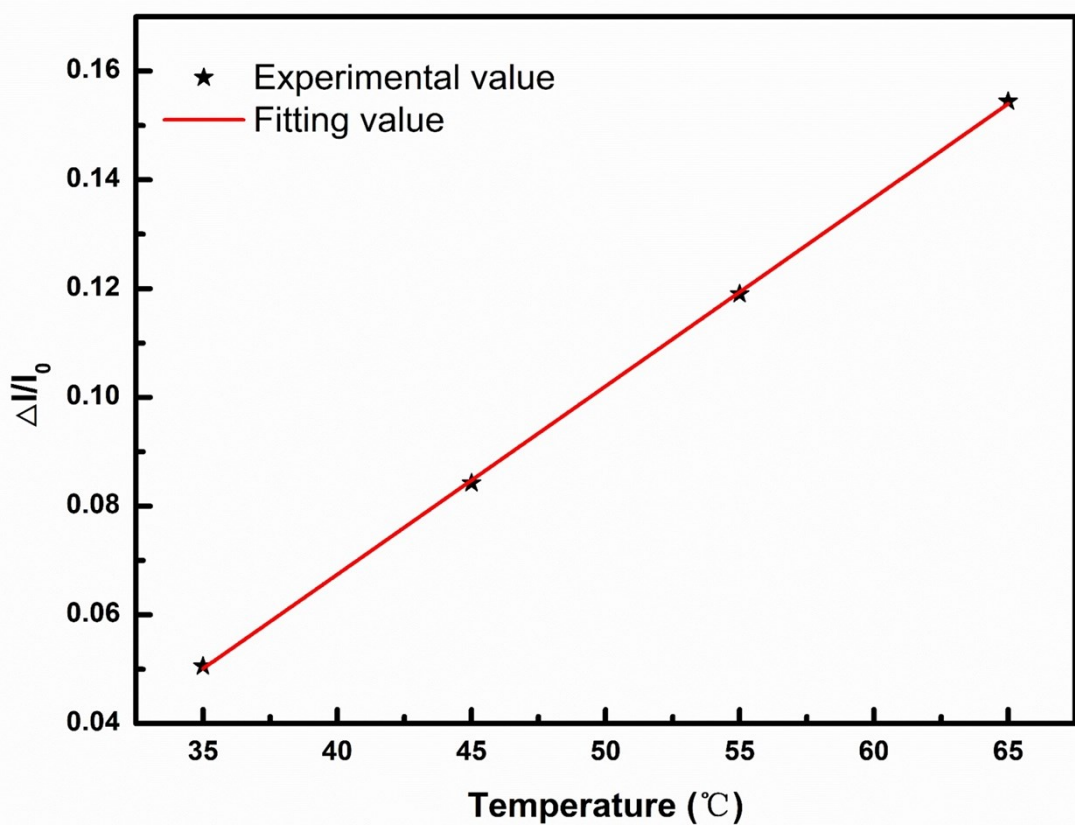


**Fig. S9** Normalized current change of RGO/CNFs/MXene-3 stimulus response sensor measured during the surface temperature between 35 and 65 °C.

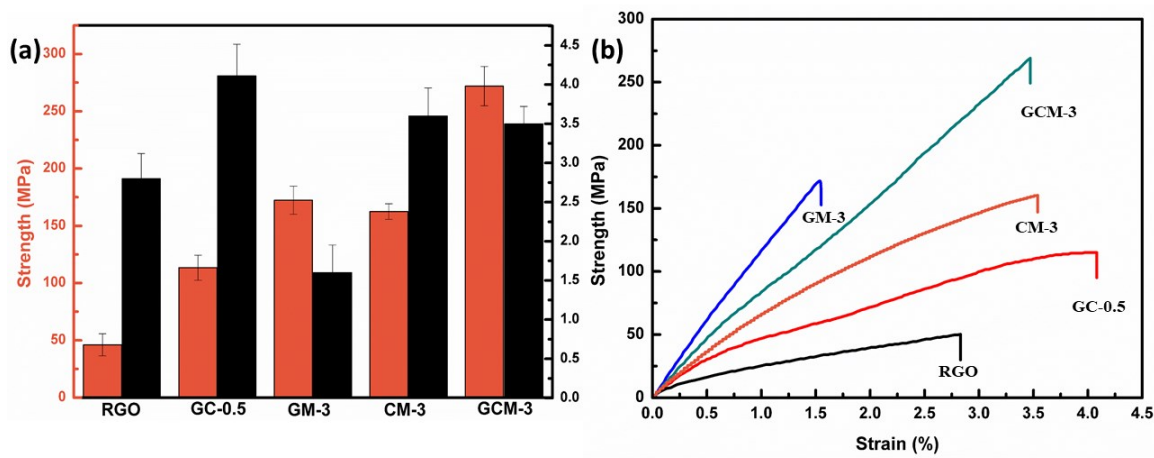


**Fig. S10** Mechanical properties of the RGO, GC-0.25, GM-3, CM-3 and GCM-3 composite paper. (a) Tensile strengths and tensile strains. (b) Tensile stress-strain curves.

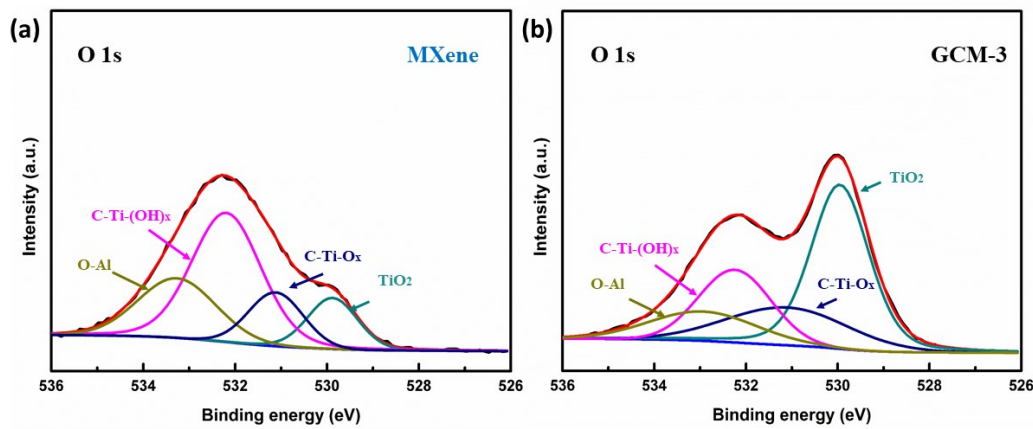


**Fig. S11** O 1s XPS spectra of MXene and RGO/CNFs/MXene-3 composite paper.

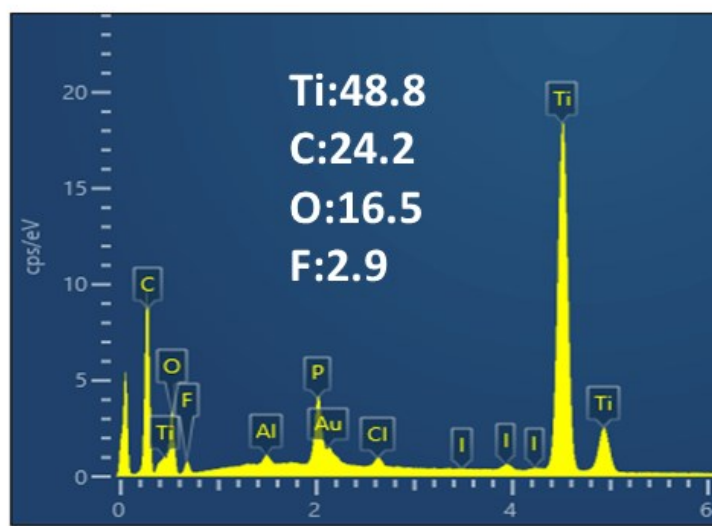


**Fig. S12** The energy spectrum analysis of an RGO/CNFs/ MXene composite paper.

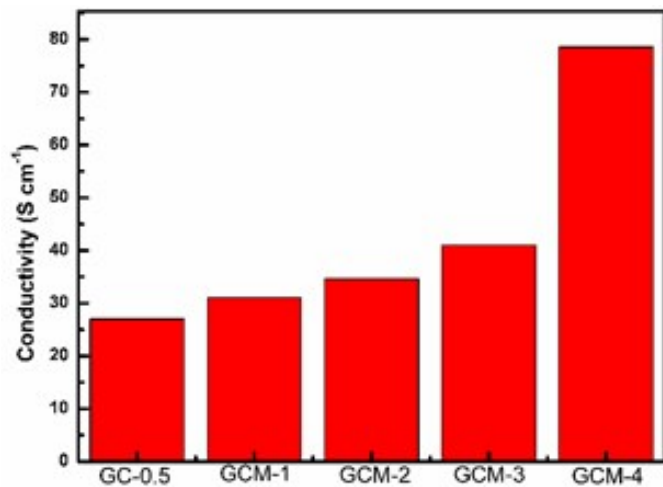


**Fig. S13** The conductivity of GC-0.5 and RGO/CNFs/ MXene composite paper.

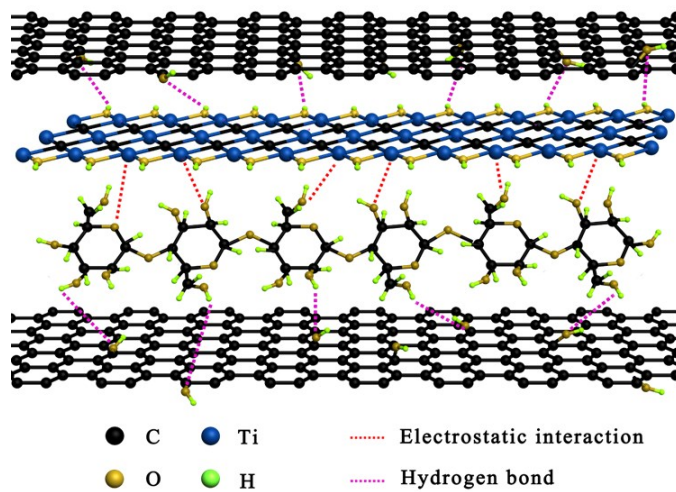


**Fig. S14** Schematic of the interaction of RGO/CNFs/MXene composite paper.

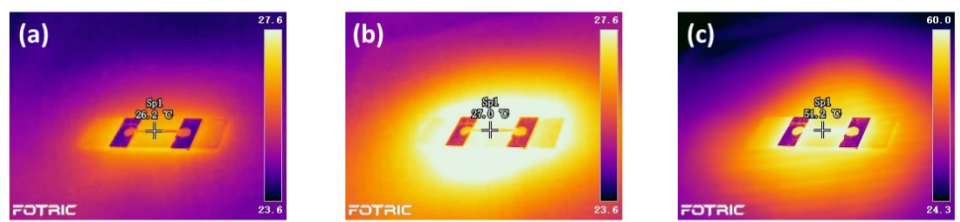


**Fig. S15** Infrared images of RGO/CNFs/MXene-3 stimulus-response sensor. (a) Under room temperature. (b) Under 365 nm light. (c) Under solar illumination.

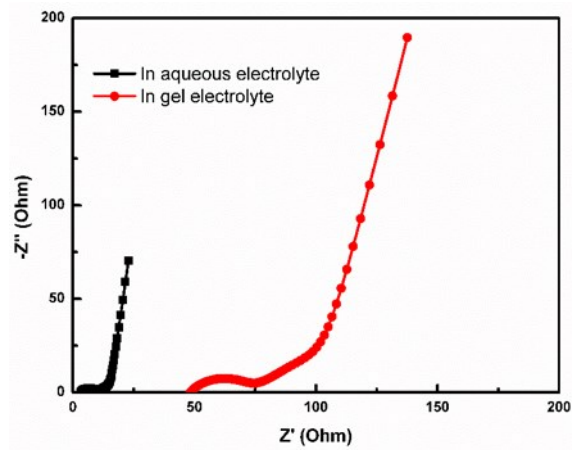


**Fig. S16** The EIS comparison of GCM-3 composite paper in different electrolyte.

**Table S1.** Several mechanical parameters of the GCM-3 composite paper compared with natural nacre and some reported energy storage materials.

Sample	Materials	Tensile		Reference
		strength (MPa)	Strain (%)	
1	MXene foam	4	0.45	[7]
2	GPs	246	0.8	[8]
3	LG	54	3.2	[9]
4	GP/TiO <sub>2</sub> -epoxy	75	1.2	[10]
5	Natural Nacre	135	0.85	[11]
6	Ti <sub>3</sub> C <sub>2</sub> T <sub>x</sub> film	22	1	[12]
7	RGO/MXene	132.5	2.9	[13]
8	RGO/Aramid	100.6	2.1	[14]
9	RGO/CNFs	8.67	3	[15]
10	RGO/PANI	12.6	0.11	[16]
11	CNT/PPy	68.73	0.65	[17]
12	GCM composite paper	238	3.9	<b>This work</b>

**Table S2** Several electrochemical parameters of the composite papers compared with some reported energy storage devices.

Electrode material	Electrolyte	E (mWh cm <sup>-3</sup> )	P (W cm <sup>-3</sup> )	Reference
PEDOT:PSS	H <sub>2</sub> SO <sub>4</sub> /PVA	1.5	0.03	[18]
RGO/CNT/CMC	H <sub>2</sub> PO <sub>4</sub> /PVA	3.5	0.018	[19]
Fe <sub>2</sub> O <sub>3</sub> /PPy	NA	0.22	0.165	[20]
Carbon fiber/MnO <sub>2</sub>	H <sub>2</sub> PO <sub>4</sub> /PVA	0.22	0.4	[21]
RGO/MoS <sub>2</sub>	H <sub>2</sub> SO <sub>4</sub> /PVA	4.15	0.021	[22]
CUO /AnPd	KOH/PVA	0.413	0.55	[23]
RGO /PVA	H <sub>2</sub> SO <sub>4</sub> /PVA	2	0.2	[24]
RGO /MXene	H <sub>2</sub> PO <sub>4</sub> /PVA	3.4	0.25	[25]
RGO/CNT	H <sub>2</sub> PO <sub>4</sub> /PVA	4.9	15.5	[26]
EG/V <sub>2</sub> O <sub>5</sub>	LiCl/PVA	18.2	235	[27]
RGO/PANI	H <sub>2</sub> SO <sub>4</sub> /PVA	11.7	2	[28]
MoS <sub>2</sub> -rGO/MWCNT	H <sub>2</sub> SO <sub>4</sub> /PVA	1	0.06	[29]
Graphene hydrogel	H <sub>2</sub> SO <sub>4</sub> /PVA	1	0.03	[30]
Cellulose/PEDOT paper	H <sub>2</sub> SO <sub>4</sub> /PVA	1	0.05	[31]
RGO/MnO <sub>2</sub> /ZnO	LiCl/PVA	0.234	0.13	[32]
Graphene/PANI paper	H <sub>2</sub> SO <sub>4</sub> /PVA	0.32	0.05	[33]
RGO/CNT	H <sub>2</sub> SO <sub>4</sub> /PVA	1.57	0.11	[34]
Ti <sub>3</sub> C <sub>2</sub> T <sub>x</sub>	H <sub>2</sub> SO <sub>4</sub> /PVA	10.4	0.075	[35]
Ti <sub>3</sub> C <sub>2</sub> T <sub>x</sub> /RGO/Quantum Dots	H <sub>2</sub> SO <sub>4</sub> /PVA	16.6	0.0375	[36]
Ti <sub>3</sub> C <sub>2</sub> T <sub>x</sub> /PEDOT:PSS	H <sub>2</sub> SO <sub>4</sub> /PVA	7.17	8.349	[37]
Ti <sub>3</sub> C <sub>2</sub> T <sub>x</sub> /RGO/MnO <sub>2</sub>	LiCl/PVA	2.13	0.008	[38]
Ti <sub>3</sub> C <sub>2</sub> T <sub>x</sub> /Fe <sub>2</sub> O <sub>3</sub>	LiCl/PVA	1.61	0.02	[39]
GCM MFSC	KOH/PVA	26.11	0.25	<b>This work</b>

**Table S3** Several sensing performances of our device compared with various pressure sensors.

Materials	Sensitivity (kPa <sup>-1</sup> )	Initial pressure (Pa)	Reference
CB@PU	0.068	91	[40]
Graphene oxide foam	15.2	200	[41]
MXene/tissue paper	3.81	10.2	[42]
Percolative metal nanoparticle arrays	0.13	0.5	[43]
Graphene-Silicon	15.9	60	[44]
PEDOT:PSS/PUD/PDMS	4.88	23	[45]
SWNT/tissue paper	2.2	35	[46]
CNT/cotton textile	14.4	2	[47]
RGO/PI	0.18	NA	[48]
Graphene aerogels	0.18	NA	[49]
Graphene/Polyurethane Sponge	0.26	NA	[50]
GCM composite paper	19.3	125	<b>This work</b>

## Reference

1. X. Xiang, Z. Yang, J. Di, W. Zhang, R. Li, L. Kang, Y. Zhang, H. Zhang and Q. Li, *Nanoscale*, 2017, **9**, 11523-11529.
2. A. K. Geim and K. S. Novoselov, *Nature Materials*, 2007, **6**, 183–191.
3. M. J. Allen, V. C. Tung and R. B. Kaner, *Chem Rev*, 2010, **110**, 132–145.
4. H. Wang, D. Li, H. Yano and K. Abe, *Cellulose*, 2014, **21**, 1505-1515.
5. M. R. Lukatskaya, O. Mashtalir, C. E. Ren, Y. Dall'Agnese, P. Rozier, P. L. Taberna, M. Naguib, P. Simon, M. W. Barsoum and Y. Gogotsi, *Science*, 2013, **341**, 1502-1505.
6. Z. Ling, C. E. Ren, M. Q. Zhao, J. Yang, J. M. Giamarco, J. Qiu, M. W. Barsoum and Y. Gogotsi, *Proc Natl Acad Sci U S A*, 2014, **111**, 16676-16681.
7. J. Liu, H. B. Zhang, R. Sun, Y. Liu, Z. Liu, A. Zhou and Z. Z. Yu, *Adv Mater*, 2017, **29**, 1702367.
8. W.L. Song, L.Z. Fan, M.S. Cao, M.M. Lu, C.Y. Wang, J. Wang, T.T. Chen, Y. Li, Z.L. Hou, J. Liu and Y.P. Sun, *J. Mater. Chem. C*, 2014, **2**, 5057-5064.
9. Y.J. Wan, P.L. Zhu, S.H. Yu, R. Sun, C.P. Wong and W.H. Liao, *Carbon*, 2017, **122**, 74-81.
10. A. Kumar, R. Anant, K. Kumar, S. S. Chauhan, S. Kumar and R. Kumar, *RSC Advances*, 2016, **6**, 113405-113414.
11. A. P. Jackson, J. F. V. Vincent, R. M. Turner, *Proc. R. Soc. B*, 1988, **234**, 415–440.
12. Z. Ling, C. E. Ren, M. Q. Zhao, J. Yang, J. M. Giamarco, J. Qiu, M. W. Barsoum and Y. Gogotsi, *Proc Natl Acad Sci U S A*, 2014, **111**, 16676-16681.
13. S. Seyedin, E. R. S. Yanza and Joselito M. Razal, *Journal of Materials Chemistry A*, 2017, **5**, 24076-24082.
14. S. R. Kwon, J. Harris, T. Zhou, D. Loufakis, J. G. Boyd and J. L. Lutkenhaus, *ACS Nano*, 2017, **11**, 6682-6690.
15. Z. Weng, Y. Su, D.W. Wang, F. Li, J. Du and H.M. Cheng, *Advanced Energy Materials*, 2011, **1**, 917-922.
16. D.W. Wang, F. Li, J. Zhao, W. Ren, Z.G. Chen, J. Tan, Z.S. Wu, I. Gentle, G. Q. Lu and H.M. Cheng, 2009, **3**, 1745-1752.
17. J. Che, P. Chen and M. B. Chan-Park, *Journal of Materials Chemistry A*, 2013, **1**, 4057.
18. N. Kurra, J. Park and H. N. Alshareef, *J. Mater. Chem. A*, 2014, **2**, 17058-17065.
19. L. Kou, T. Huang, B. Zheng, Y. Han, X. Zhao, K. Gopalsamy, H. Sun and C. Gao, *Nat Commun*, 2014, **5**, 3754.
20. L. Wang, H. Yang, X. Liu, R. Zeng, M. Li, Y. Huang and X. Hu, *Angewandte Chemie International*

Edition, 2017, **56**, 1105-1110.

21. X. Xiao, T. Li, P. Yang, Y. Gao, H. Jin, W. Ni, W. Zhan, X. Zhang, Y. Cao, J. Zhong, L. Gong, W.C. Yen, W. Mai, J. Chen, K. Huo, Y.L. Chueh, Z. L. Wang and J. Zhou, *ACS Nano*, 2012, **6**, 9200- 9206.
22. G. Sun, J. Liu, X. Zhang, X. Wang, H. Li, Y. Yu, W. Huang, H. Zhang and P. Chen, *Angew Chem Int Ed Engl*, 2014, **53**, 12576-12580.
23. Z. Yu and J. Thomas, *Advanced Materials*, 2014, **26**, 4279-4285.
24. S. Chen, W. Ma, H. Xiang, Y. Cheng, S. Yang, W. Weng and M. Zhu, *Journal of Power Sources*, 2016, **319**, 271-280.
25. H. Li, Y. Hou, F. Wang, M. R. Lohe, X. Zhuang, L. Niu and X. Feng, *Advanced Energy Materials*, 2017, **7**, 1601847.
26. W. Ma, M. Li, X. Zhou, J. Li, Y. Dong and M. Zhu, *ACS Appl Mater Interfaces*, 2019, **11**, 9283-9290.
27. M. Zhu, Y. Huang, Y. Huang, H. Li, Z. Wang, Z. Pei, Q. Xue, H. Geng and C. Zhi, *Advanced Materials*, 2017, **29**, 1605137.
28. Z. S. Wu, K. Parvez, S. Li, S. Yang, Z. Liu, S. Liu, X. Feng, K. Müllen, *Advanced Materials*. 2015, **27**, 4054.
29. G. Sun, X. Zhang, R. Lin, J. Yang, H. Zhang and P. Chen, *Angew Chem Int Ed Engl*, 2015, **54**, 4651-4656.
30. Y. Xu, Z. Lin, X. Huang, Y. Liu, Y. Huang and X. Duan, *ACS Nano*, 2013, **7**, 4042- 4049.
31. B. Anothumakkool, R. Soni, S. N. Bhange and S. Kurungot, *Energy & Environmental Science*, 2015, **8**, 1339-1347.
32. W. Zilong, Z. Zhu, J. Qiu and S. Yang, *J. Mater. Chem. C*, 2014, **2**, 1331-1336.
33. B. Yao, L. Yuan, X. Xiao, J. Zhang, Y. Qi, J. Zhou, J. Zhou, B. Hu and W. Chen, *Nano Energy*, 2013, **2**, 1071-1078.
34. D.Y. Wu, W.H. Zhou, L.Y. He, H.Y. Tang, X.H. Xu, Q.S. Ouyang and J.J. Shao, *Carbon*, 2020, **160**, 156-163.
35. D. Lin, O. Qian, D. Huo, Q. Pan, S. Zhang, Z. Wang, F. Han and B. Wei, *Nano Energy*, 2020, **78**, 105323.
36. X. Zhou, Y. Qin, X. He, Q. Li, J. Sun, RGO/Quantum Dots Z. Lei and Z. H. Liu, *ACS Appl Mater Interfaces*, 2020, **12**, 11833-11842.
37. J. Zhang, S. Seyedin, S. Qin, Z. Wang, S. Moradi, F. Yang, P. A. Lynch, W. Yang, J. Liu, X. Wang and J. M. Razal, *Small*, 2019, **15**, e1804732.
38. M. Lu, Z. Zhang, L. Kang, X. He, Q. Li, J. Sun, R. Jiang, H. Xu, F. Shi, Z. Lei and Z.-H. Liu, *Journal of Materials Chemistry A*, 2019, **7**, 12582-12592.

39. F. Li, Y.L. Liu, G.G. Wang, H.Y. Zhang, B. Zhang, G.Z. Li, Z.P. Wu, L.Y. Dang and J.C. Han, *Journal of Materials Chemistry A*, 2019, **7**, 22631-22641.
40. X. Wu, Y. Han, X. Zhang, Z. Zhou, C. Lu, *Advanced Functional Materials*, 2016, **26**, 6246-6256.
41. C. Hou, H. Wang, Q. Zhang, Y. Li, M. Zhu, *Advanced Functional Materials*, 2014, **26**, 5018-5024.
42. Y. Guo, M. Zhong, Z. Fang, P. Wan and G. Yu, *Nano Lett*, 2019, **19**, 1143-1150.
43. M. Chen, W. Luo, Z. Xu, X. Zhang, B. Xie, G. Wang and M. Han, *Nature Communications*, 2019, **10**, 4024.
44. N. Luo, Y. Huang, J. Liu, S. C. Chen, C. P. Wong and N. Zhao, *Advanced Materials*, 2017, **29**, 1702675.
45. C.L. Choong, M.B. Shim, B.S. Lee, S. Jeon, D.S. Ko, T.H. Kang, J. Bae, S. H. Lee, K.E. Byun, J. Im, Y. J. Jeong, C. E. Park, J.J. Park and U. I. Chung, *Advanced Materials*, 2014, **26**, 3451- 3458.
46. Z. Zhan, R. Lin, V. T. Tran, J. An, Y. Wei, H. Du, T. Tran and W. Lu, *Acs Applied Materials & Interfaces*, 2017, **9**, 37921-37928.
47. M. Liu, X. Pu, C. Jiang, T. Liu, X. Huang, L. Chen, C. Du, J. Sun, W. Hu and Z. L. Wang, *Advanced Materials*, 2017, **29**, 1703700.
48. Y. Qin, Q. Peng, Y. Ding, Z. Lin, C. Wang, Y. Li, F. Xu, J. Li, Y. Yuan, X. He, Y. Li, *ACS Nano*, 2015, **9**, 8933.
49. C. Li, D. Jiang, H. Liang, B. Huo, C. Liu, W. Yang, J. Liu, *Advanced Functional Materials*, 2018, **28**, 1704674.
50. H. B. Yao, J. Ge, C. F. Wang, X. Wang, W. Hu, Z. J. Zheng, Y. Ni, S. H. Yu, *Advanced Materials*, 2013, **25**, 6691.